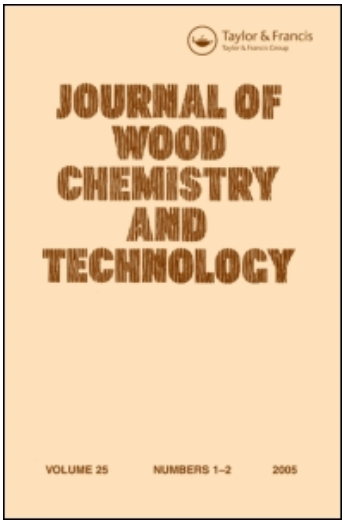

Journal of Wood Chemistry and Technology
Publication details, including instructions for authors and subscription information:
http://www.informaworld.com/smpp/title~content=t713597282

Analysis of Among-Species Variability in Wood Fiber Surface Using DRIFTS and XPS: Effects on Esterification Efficiency

Hassine Bouafif[a]; Ahmed Koubaa[a]; Patrick Perré[b]; Alain Cloutier[c]; Bernard Riedl[c]
[a] Département des Sciences Appliquées, Université du Québec en Abitibi-Témiscamingue, Rouyn-Noranda, Québec, Canada [b] AgroParisTech, INRA, Nancy, France [c] Centre de Recherche sur le Bois, Université Laval, Québec, Canada

To cite this Article Bouafif, Hassine , Koubaa, Ahmed , Perré, Patrick , Cloutier, Alain and Riedl, Bernard(2008) 'Analysis of Among-Species Variability in Wood Fiber Surface Using DRIFTS and XPS: Effects on Esterification Efficiency', Journal of Wood Chemistry and Technology, 28: 4, 296 — 315
To link to this Article: DOI: 10.1080/02773810802485139
URL: http://dx.doi.org/10.1080/02773810802485139

Journal of Wood Chemistry and Technology, 28: 296–315, 2008

ISSN: 0277-3813 print / 1532-2319 online
DOI: 10.1080/02773810802485139

Taylor & Francis
Taylor & Francis Group

Analysis of Among-Species Variability in Wood Fiber Surface Using DRIFTS and XPS: Effects on Esterification Efficiency

Hassine Bouafif,[1] Ahmed Koubaa,[1] Patrick Perré,[2] Alain Cloutier,[3] and Bernard Riedl[3]

[1]Département des Sciences Appliquées, Université du Québec en Abitibi-Témiscamingue, Rouyn-Noranda, Québec, Canada
[2]AgroParisTech, INRA, UMR1093, LERMAB, Nancy, France
[3]Centre de Recherche sur le Bois, Université Laval, Québec, Canada

Abstract: Variability in the chemical composition of surface properties of various wood fibers (eastern white cedar, jack pine, black spruce, and bark) was investigated using diffuse reflectance infrared Fourier transform spectroscopy (DRIFTS) and X-ray photoelectron spectroscopy (XPS). Both DRIFTS and XPS showed high variability in fiber surface composition between species and between fiber types (sapwood, heartwood, and bark). Fiber surface was modified by esterification reaction using a maleic anhydride polyethylene (MAPE) treatment. DRIFTS failed to assess surface modification, whereas XPS results showed that MAPE treatment increased the surface hydrocarbon concentration of jack pine wood fiber, indicated by a decrease in oxygen–carbon ratio and an increase in relative intensity of the C1 component in the C1s signal. Lignin concentration variability on the fiber surface was determined as the major factor that prevents esterification from taking place.

Keywords: Coupling agent, DRIFTS, esterification, surface analysis, wood fiber, XPS

INTRODUCTION

Surface chemical properties of wood play an important role in fiber-to-fiber adhesion and fiber adhesion to thermoplastic and thermoset polymers.[1] However, the variability of wood chemical composition in the fiber cell wall and on the

The authors are grateful to the Canada Research Chair Program, Quebec's Ministère du Développement économique, Innovation et Exportation (MDEIE), Institut Français de coopération de Tunisie (IFC), Caisse Populaire Desjardins, Tembec, La Fondation de l'UQAT, and Dr. A. Adnot for scientific contribution.

Address correspondence to Hassine Bouafif, Departement des Sciences Appliquées, Université du Québec en Abitibi-Témiscamingue, 445 BD de l'Université, Rouyn-Noranda, (QC) Canada, J9X5E4. E-mail: Hassine.bouafif@uqat.ca

fiber surface is very high. The main components of wood are cellulose, hemicelluloses, and lignin fractions, which vary widely among and within species.[1] Hemicelluloses are known as the main sites of interaction with water for hydrogen bonding due to their greater accessibility.[1] Lignin and other extractives (phenolic-OH) found in wood act as antioxidants through resonance stabilization of free radicals, thus inhibiting grafting and copolymerization.[2]

The surface properties of wood fibers are dependent not only on intrinsic characteristics of wood species but also on the method of preparation. For instance, mechanical and thermomechanical fiber separations usually display lignin-rich fiber surfaces, while chemical separation processes result in carbohydrate-rich surfaces.[3] The surface tension of chemically produced fibers is often higher than that of mechanically produced fibers.[4] Subsequently, the functional groups, on the surface of chemically produced fibers, are capable of stronger secondary interactions with other polymers, such as reported for polyolefins.[5]

Several studies have focused on the effect of lignin content on wood-based composite properties. Luo et al.[6] studied the effect of high lignin content on HDPE/lignin composites. They found that elongation at break of the composites gradually increased with lignin content. Bending modulus and bending strength increased with lignin dosage by 17.3% and 12.2%, respectively. They also observed that bending strength reached a maximum value of 16.1 MPa at the lignin mass fraction of 2.5%, and subsequently declined with increasing lignin dosage, whereas tensile strength of the HDPE/lignin composite increased by 8.0%.

Similarly, Le Digabel and Avěrous[7] noted a decrease in stress at the limit of elasticity with increasing lignin content, whereas elongations at break and at the yield point increased with lignin content. Nevertheless, they concluded that the increased moduli in the biocomposites were mainly caused by cellulose filler rather than lignin content.

Although extractives constitute a small weight percentage of the chemical composition, they dominate the surface chemistry of wood fibers. Depending on chemical nature and concentration, extractives are considered as surface contaminants, with deleterious effects on wood–polymer compatibility. Saputra and co-workers[8] investigated how the removal of extractives from pine and Douglas fir can affect the mechanical properties of wood–polypropylene (PP) composites, and they reported that mixing wood flour or wood fibers and thermoplastics at high temperatures allowed extractives to migrate to the wood flour surface and accumulate in the wood–plastic interphase. Subsequent removal of this weak boundary layer led to a significant improvement in interfacial shear strength between the polypropylene matrix and the extracted wood filler.[8]

Poor interfacial bonding and weak compatibility between wood-based materials and the most commonly used polymers are by far the greatest limiters of wood–plastic composite (WPC) applications. Because polymers

and wood fillers are incompatible, certain surface modifications, mostly using coupling agents, are required to improve the service performance of composites.[9–12] Maleic anhydride grafted polyethylene and maleic anhydride grafted polypropylene (MAPE and MAPP, respectively) are mostly used as coupling agents in extruded WPC or lignocellulosic-based composite materials performed in liquid phase.[13–14]

Although all researchers agree on the need to make changes to the surface of wood fillers, there is a lack of consensus on the effects of concentration and type of functionalized polymer on composite properties. Lu et al.[11] observed that tensile strength and flexural storage moduli pass through a maximum as a function of concentration of the coupling agent. Similar behavior was also observed by Sombatsompop et al.[14] at low concentration. However, others authors have found that composite stiffness was not significantly influenced by the presence of the functionalized polymer, and only strength was considerably increased.[10,15]

Compared to the number of studies on coupling mechanisms and interfacial characterization, few studies have investigated the effects of the intrinsic characteristics of wood fillers according to wood species and type (sapwood, heartwood, and bark-based particles).

This study investigates between-species variability in wood fiber surface composition by spectral characterization using Diffuse Reflectance Fourier Transform Infrared Spectroscopy (DRIFTS) and X-ray photoelectron spectroscopy (XPS). Variations in the grafting efficiency of maleic anhydride polyethylene with wood species and type are also discussed.

EXPERIMENTAL

Five types of wood particles were used in this study: eastern white cedar (*Thuya occidentalis*), jack pine (*Pinus banksiana* Lamb.), bark (jack pine), and black spruce (*Picea mariana* (mill)). Because these species are widely used in eastern Canada for lumber production, they generate considerable quantities of lignocellulosic residues (shaving, sawdust, and bark). All ligno-cellulosic materials were obtained from a softwood sawmill located in Abitibi-Temiscaming in western Quebec, Canada. Wood sawdust and bark shavings were ground in a hammer mill and sieved into several size groups. At this stage, the moisture content of the particles was 10.5%. Particles were not extracted. In addition, bleached Kraft pulp fibers were used as a control.

Ethylene-maleic anhydride copolymers (MAPE, A-C® 575A), supplied by Honeywell (Minneapolis, Minnesota), was used to graft the wood and bark fibers. It has a specific gravity of 0.92 and a 104–107°C melting point.

MAPE grafting of wood flour (42 mesh) was conducted in a reactor in the presence of a solvent according to the method described by Kazayawoko et al.[16,17] and Chuai et al.[18] Before grafting, the wood flour was oven-dried

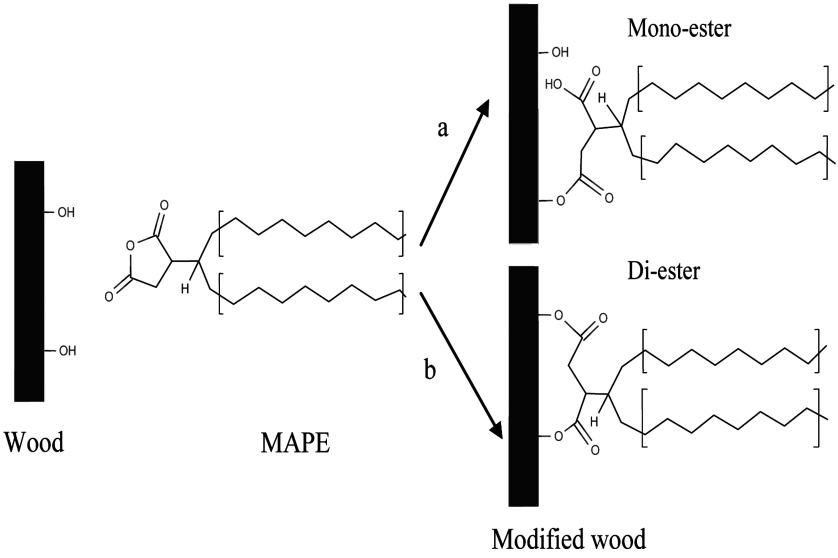

Figure 1. Model of the esterification reaction between wood fiber and maleic anhydride polyethylene.[19]

at 105°C for 24 h. The reaction procedure used to modify the wood flour was as follows: 250 ml of xylene was placed in a 500 ml reactor and stirred continuously to 130–140°C, at which point 5 g of MAPE (A-C® 575A) and 30 g of wood flour were placed in the reactor. One gram of sodium hypophosphite hydrate was added as an esterification catalyst. The reaction was carried out for 2 h at 130–140°C. As shown in the reaction schematic (Figure 1), two reactions were possible between MAPE and wood particles: a single site reaction, which led to monoester formation in addition to the carboxylic acid groups (Figure 1a); or diester formation without the carboxylic acid groups (Figure 1b).[19] After the reaction, the mixture was filtered to isolate the reacted wood flour. The treated wood flour was treated by soxhlet extraction with xylene for 8 h to remove the unreacted anhydride, then oven-dried at 70°C for 24 h.

Diffuse reflectance infrared Fourier transform spectroscopy (DRIFTS) was performed in order to: (i) provide detailed information on the functional groups present at the surface of the wood particle samples; and (ii) confirm whether esterification reaction occurred between wood flour and maleic polyethylene. DRIFTS was conducted on a Tensor 27 FT-IR system (Bruker Optics, Germany) equipped with a deuterated triglycine sulfate (DTGS) detector. For each sample, spectra were recorded by collecting 164 scans in the range of 4000–400 cm^{-1} at 4 cm^{-1} resolution. Pure powdered potassium bromide (KBr) was used as a reference substance. Since the DRIFTS spectra of wood powders in KBr are substantially influenced by both particle size and concentration,[20] samples for DRIFTS were carefully prepared in microcups as follows: 1 mg of each wood

flour (100 mesh) was mixed with KBr in the proportion of 1/100 (% by weight) in an agathe mortar and then transferred to a 4-mm diameter cup where it was lightly compressed and leveled using a spatula. Tilted baselines of the original spectra were not altered.

X-ray photoelectron spectroscopy (XPS) was also used for surface analyses of the wood and bark samples. Prior to XPS analysis, samples were oven-dried. XPS spectra of unmodified and modified wood flour were recorded with an X-ray photoelectron spectrometer (Kratos Axis Ultra, UK). All spectra were collected using a monochromatic Al Kα X-ray source (1486.6 eV). The lateral dimensions of the samples were 800 microns $\times$ 400 microns, corresponding to those of the Al Kα X-ray used, and probing depth was approximately 5 nanometers. For each sample, two spectra in the fixed analyzer mode were recorded: (i) survey spectra (0–1150 eV and pass energy 120 eV) were recorded to estimate composition; and (ii) high-resolution spectra (within 20 eV and pass energy 20 eV) were recorded to obtain information on chemical bonds.

From the survey spectra, the atomic concentration ratio of oxygen to carbon was determined by integrating the area under the curve after removal of the linear background.[21–23] High-resolution analysis of the carbon chemical bonds was performed by iterative convolution, using a nonlinear least-squares procedure based on the Levenberg-Marquardt algorithm. Peak synthesis was performed with CasaXPS. Peak intensities at a given bending energy were generated as a Gauss-Lorentz product function peak. The Gauss-Lorentzian ratio was set at 0.30 for all curve fittings.

RESULTS AND DISCUSSION

Surface and Interface Characterization by DRIFTS

FTIR Spectra of Untreated Wood Fibers

Figure 2 shows the FTIR absorption spectra of untreated wood particles for different species in the 4000 and 400 cm^{-1} range. Bleached Kraft fibers were included to provide more information.

Because bark and wood have similar chemical compositions, the bark absorption bands were assigned to specific chemical functions analogous to those of wood.[24] Although an overview of all wood samples shows similar IR spectra, high-resolution analysis reveals several divergences in the fingerprint region of the spectra (<1500 cm^{-1}). Differences are observed mainly between the bark spectrum and the rest of the wood spectra.

Spectra of the untreated wood particles show the presence of a broad stretching band for intermolecular bonded hydroxyl groups at 3400 cm^{-1}. The OH groups may include absorbed water, aliphatic primary and secondary alcohols found in carbohydrates and lignin, aromatic primary and secondary

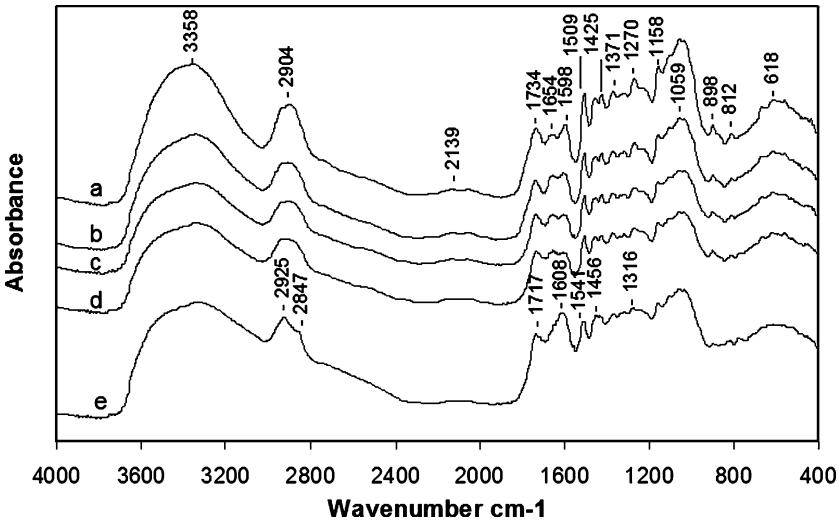

Figure 2. FTIR spectra of untreated fibers: eastern white cedar; heartwood (a) and sapwood fibers (b), jack pine wood fibers (c), black spruce wood fibers (d), and jack pine bark fibers (e).

alcohols in lignin and extractives, and carboxylic acids in extractives.[17,20,25] This OH stretching band is flanked by prominent methylene/methyl bands appearing at 2904 cm^{-1}. In the case of bark particles, these bands are shifted and divided into two peaks at 2925 cm^{-1} and 2847 cm^{-1}, respectively.

A broad, medium intensity ester carbonyl vibration appears at 1735 cm^{-1}, which is presumed to emanate from carbonyl (C=O) stretching of acetyl groups in hemicelluloses and carbonyl aldehyde in lignin and extractives.[25–28] Kazayawoko and co-workers[17] also attributed this vibration to carbonyl (C=O) stretching of carboxyl groups in hemicelluloses, lignin, and extractives, as well as esters in lignin and extractives. In the case of the particle bark spectrum, weak carboxylic carbonyl functionality at 1717 cm^{-1} is superimposed as a shoulder, with a broad carbonyl band appearing at 1735 cm^{-1}. The bands around 1608 cm^{-1} and 1510 cm^{-1} can also be distinctly identified due to the aromatic C=C skeletal vibrations mainly linked to the lignin structure.[29–35]

In the fingerprint region between 1600 and 400 cm^{-1}, many sharp and discrete absorption bands due to various functional groups present in the wood constituents are observed. The medium intensity bands around 1456 cm^{-1}, 1425 cm^{-1}, and 1371 cm^{-1} are associated with methylene deformation and methyl asymmetric and methyl symmetrical vibrations.[17,20,25,36] The broad, strong bands appearing at 1270 cm^{-1} are due to either a carbon single bonded oxygen stretching vibration or an interaction vibration between carbon single

bonded oxygen stretching and in-plane carbon single bonded hydroxyl bend in carboxylic acids.[36]

Papp et al.[35] attributed bands containing no other nearby absorption maxima to one chemical component (1510 cm^{-1}: aromatic rings, 1270 cm^{-1}: guaiacyl units, 1158 cm^{-1}: C–O–C bonds in the cellulose). The observed absorption band at 1158 was identified as a result of the asymmetric stretching of C—O—C in the cellulose and hemicelluloses.[17,37] However, Ajuong and Breese[36] suggested that this medium intensity absorption may arise from saturated fatty acid ester carbon single bonded oxygen stretching, in association with the ester carbonyl discussed earlier at lower wavenumber. Strong intensity bands at 1059 cm^{-1} and 1036 cm^{-1} are essentially in the positions corresponding to those observed by Chen and Jakes[38] in the IR spectra of single cotton fibers. Finally, the vibrations appearing further down the field at 898 cm^{-1} and 812 cm^{-1} may arise from disubstituted ring stretching and out-of-plane carbon single bonded hydrogen.[36]

DRIFTS was used as a semi-quantitative method to compare the chemical composition of the untreated wood particle surfaces. The following bands were selected as the most characteristic: (1) 1735 cm^{-1} for lignin and extractives; (2) 1605 cm^{-1} and 1510cm^{-1} for lignin and aromatic skeletal components; (3) 1271 and 1231 cm^{-1} for guaiacyl units of lignin; and (4) 1158 cm^{-1} for fatty acids. Figure 3 shows the area under peak, without linear background, of the selected band spectra for wood. It confirms the variability of particle surface, not only between species, but also within tree types (sapwood vs. heartwood).

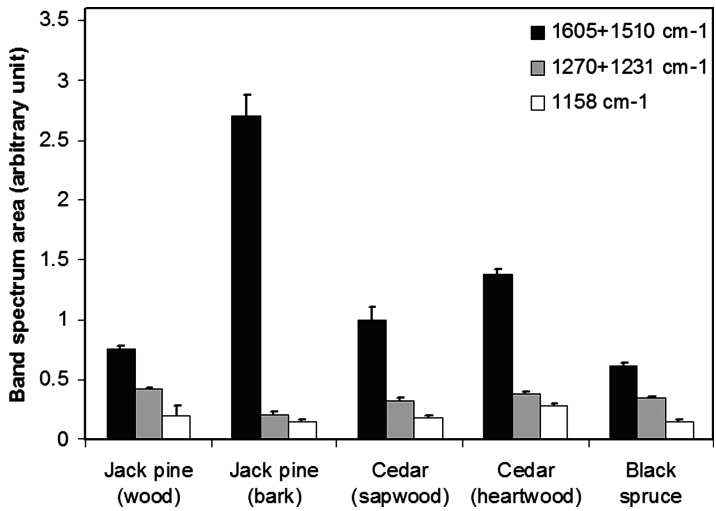

Figure 3. Area under the peak of the most important absorption band spectra of the studied wood and bark fibers.

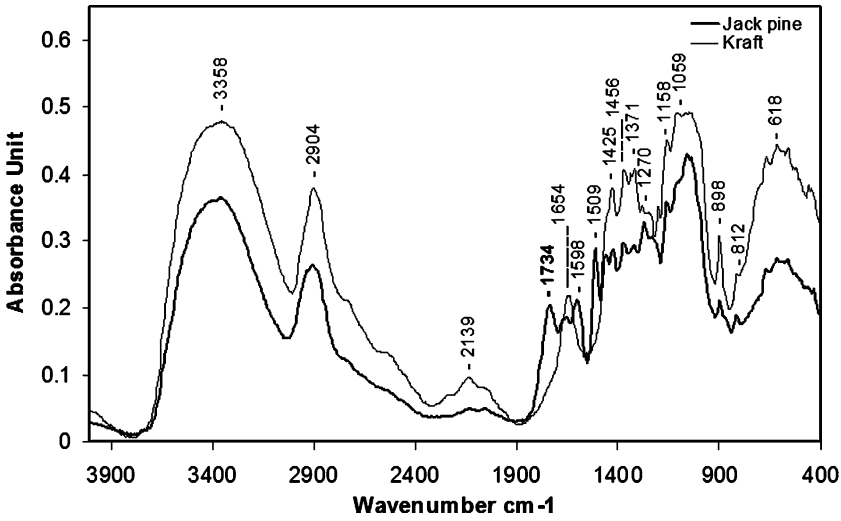

Figure 4. FTIR spectra of bleached Kraft versus untreated jack pine fibers.

The FTIR spectra of untreated wood were compared with those of bleached Kraft fibers. Figure 4 shows the FTIR spectra of untreated jack pine wood and bleached Kraft fibers. As can be seen, the greatest differences are located around 1735 cm^{-1}, which, as discussed earlier, may be linked to carbonyl (C=O) stretching of carboxyl groups in hemicelluloses, lignin, and extractives and/or to esters in lignin and extractives. This absorption band is absent in the FTIR spectra of bleached Kraft fibers. The observed absorption band at 1647 cm^{-1} arises when the semi-acetal hydroxyl group of the cellulose molecule transforms into aldehyde.[26] However, others studies have assigned this vibration to absorbed water.[10,17]

FTIR Spectra of Maleic Anhydride Polyethylene

Figure 5 shows the MAPE absorption spectra (MAPE, A-C® 575A). The most characteristic assignments of absorption bands are presented in Table 1. The strong intensity bands at 2920 cm^{-1} and 2851 cm^{-1} are characteristic of CH_2 stretching vibrations in polyethylene chains. The vibration at 1772 is associated with the anhydre carbonyl (C=O) symmetric and asymmetric stretching, while bands near 1716 may be assigned to carbonyl stretching vibrations of carboxyl groups.[10,19,39]

Comparison Between Treated and Untreated Fiber Surfaces

The digital subtraction of the FTIR wood spectra after and before treatment with MAPE did not indicate the presence of any distinctive absorption bands around

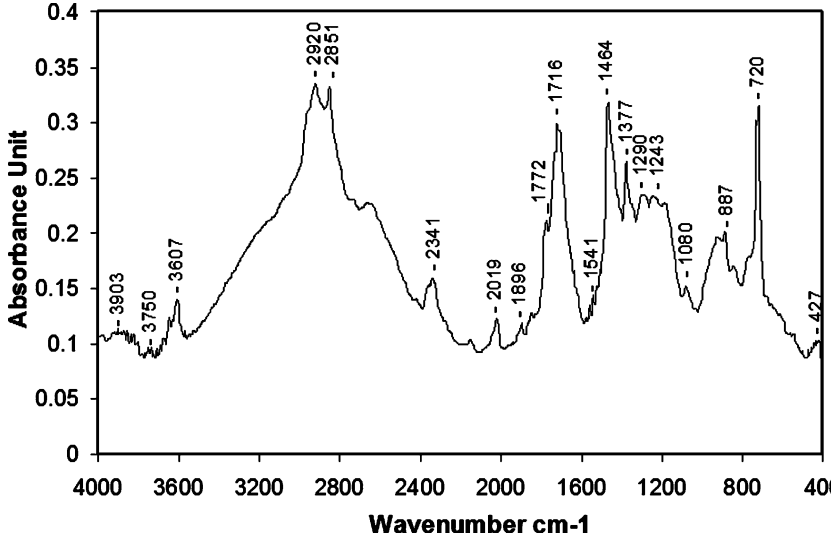

Figure 5. FTIR spectra of pure maleic anhydride polyethylene (MAPE, A-C® 575A).

1735 cm^{-1} that may be assigned to ester bonds between hydroxyl groups of wood fibers and maleic anhydride polyethylene. However, the peak around 1740 cm^{-1} confirms an effective esterification reaction between hydroxyl groups of bleached Kraft fibers and anhydride groups of the MAPE.

Although DRIFTS was successfully used to characterize the main chemical bonds on the fiber surface, it failed to confirm esterification between wood particles and maleated polyethylene. This could be explained by many factors. (i) The C=O bonding resulting from esterification can be overlapped by those already present in extractives and lignin. (ii) The sensitivity of DRIFTS limits measurement reproducibility and repeatability. Faix and Böttcher[20] found that carbohydrate intensities, mainly around 1100 cm^{-1}, are strongly influenced by

Table 1. FTIR absorption bands and assignments of pure MAPE[10,19]

Wave number (cm^{-1})	Assignment
2920–2851	CH stretching of CH_2, CH_3
1772	Anhydride C=O stretching
1716	C=O stretching (carboxyl group)
1464	CH_2 deformation
1377	CH_2 deformation
720	$(CH_2)_n$ rocking vibration ($n > 3$)

variations in wood concentration in the dispersing KBr matrix and the particle size of the milled wood. Otherwise, in the wavenumber range above 1150 cm^{-1}, intensity depends solely on the content of the chemical components.[25] This may explain why researchers have often been interested in this wave range when characterizing the chemical composition of lignocellulosic materials.[27,40–45] (iii) The vibration intensity of each selected component depends on which part of the fiber surface has been scanned. In other words, it depends on how the fiber wall was fractured during mechanical grinding or milling. Many surface types are created, because the cracks in the fibers are usually related to the stiffness of the cell wall, and especially the thickness of the S2 layer, which depends on wood species and type.

Surface and Interface Characterization by XPS

Typical XPS spectra for eastern white cedar, bark, and bleached Kraft fibers are shown in Figure 6. As expected, in all spectra, only oxygen and carbon can be clearly identified. However, relatively weak peaks of other major elements such as nitrogen, silicon, magnesium, phosphor, and calcium are also observed, possibly arising from sites during tree growth or from contamination during sample preparation. In the case of bleached Kraft, the presence of mineral elements can be attributed to residual magnesium salts and sodium silicate, which are frequently added to improve bleaching with alkaline peroxide. The survey spectra of the other wood species (black spruce and jack pine) exhibit similar trends to eastern white cedar.

The atomic concentration ratio of oxygen to carbon (O/C) was used as an initial indication of surface oxidation (Table 2). The O/C atomic ratio for eastern white cedar fibers and black spruce fibers is equal (0.28), while jack pine fibers show the most oxidized unmodified surface (0.35). Bark fibers show the lowest O/C ratio (0.18) and bleached Kraft fibers exhibit by far the highest O/C ratio (0.72). The difference in O/C ratio has been shown to be proportional to the amount of lignin on the sample surface.[21,22]

The C1s signal is usually deconvoluted into four components according to oxidation level (Table 3): C1 refers to unoxidized carbon (i.e., C–C and/or C–H), C2 corresponds to carbon with one bond to oxygen (i.e., O—C), C3 is assigned to carbon with two bonds to oxygen (i.e., O—C—O and C═O), and C4 refers to carbon with three bonds to oxygen (i.e., O—C═O). C2 and C3 components arise mainly from carbohydrates, and C1 and C4 components arise mainly from lignin and wood extractives. Area percentages of the three C1s components are shown (Table 2) for treated and untreated samples. The binding energy values of C1, C2, C3, and C4, which correspond, respectively, to 285 $\pm$ 0.01 eV, 286.6 $\pm$ 0.1 eV, 288 $\pm$ 0.3, and 289 $\pm$ 0.6 eV, are in good agreement with those reported in the literature.[21,22,46,47]

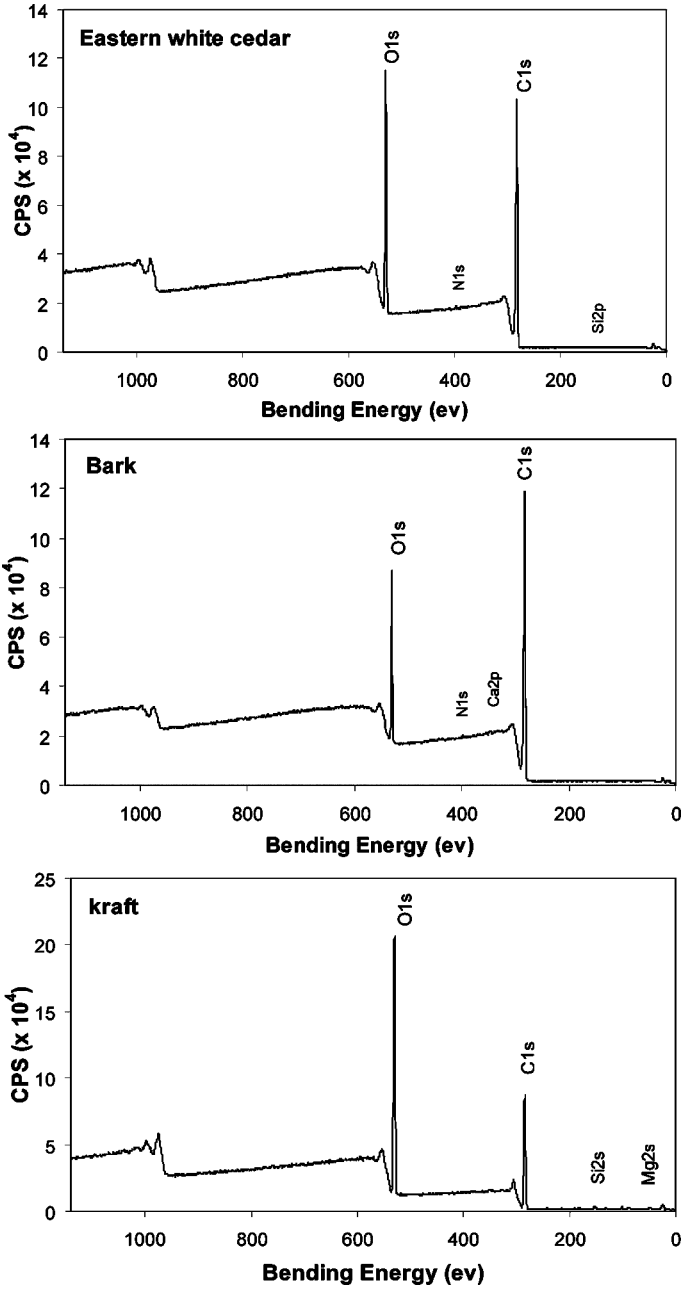

Figure 6. X-ray Photoelectron spectroscopic (XPS) survey spectra of different unmodified wood fibers.

Table 2. Analysis of O/C atomic ratio and high resolution C1s peaks of untreated and treated wood fibers

		C1s			
	O/C	C1	C2	C3	C4
Bleached Kraft	0.72	13.7	64.7	17.1	3.9
Bleached Kraft (treated)	0.26	65.1	25.9	6.5	2.6
Eastern white cedar	0.28	60.8	32.8	4.8	1.6
Eastern white cedar (treated)	0.31	58.9	31.6	6.0	3.5
Jack pine	0.35	48.2	37.9	9.7	4.2
Jack pine (treated)	0.28	63.1	27.7	5.4	3.9
Black spruce	0.28	59.5	30.0	6.9	3.6
Black spruce (treated)	0.30	58.2	31.3	6.2	4.2
Bark	0.18	69.5	21.4	5.6	3.5
Bark (treated)	0.23	66.9	23.0	5.9	4.1

The significant contribution of C2 supports the results from the O/C ratio, suggesting that bleached Kraft fibers are delignified. Thus, exposed surface is essentially rich in carbohydrates, with high content in hydroxyl groups. The lower C1 content in bleached Kraft fiber surfaces arose from the residual lignin. However, assuming that all fatty acids and glycerides were entirely removed during the Kraft pulping process and no contamination occurred during sample preparation, the presence of the C4 class of carbon atoms can be attributed to acetyl groups of hemicelluloses content.[48] On the other hand, the low O/C atomic ratio, the significant contribution of C1, and the presence of the C4 class, which were mainly observed in bark fibers, indicate that extractives such as fatty acids and resinic acids govern surface composition.

Table 3. Classification of carbon peak components (C1s) for wood fibers

Carbon atom class	Bending energy (eV)	Oxidation level	Main wood component	References
C1	285 ± 0.01	C—C and/or C—H	Terpenes, Fatty acids, lignin	[22, 47, 49]
C2	286.6 ± 0.1	C—O	Celluloses, hemicelluloses, and lignin	[49]
C3	288 ± 0.3	C═O and/or O—C═O	Fatty acids and their esters	[22]
C4	289 ± 0.6	O—C═O	Resinic acids	[22]

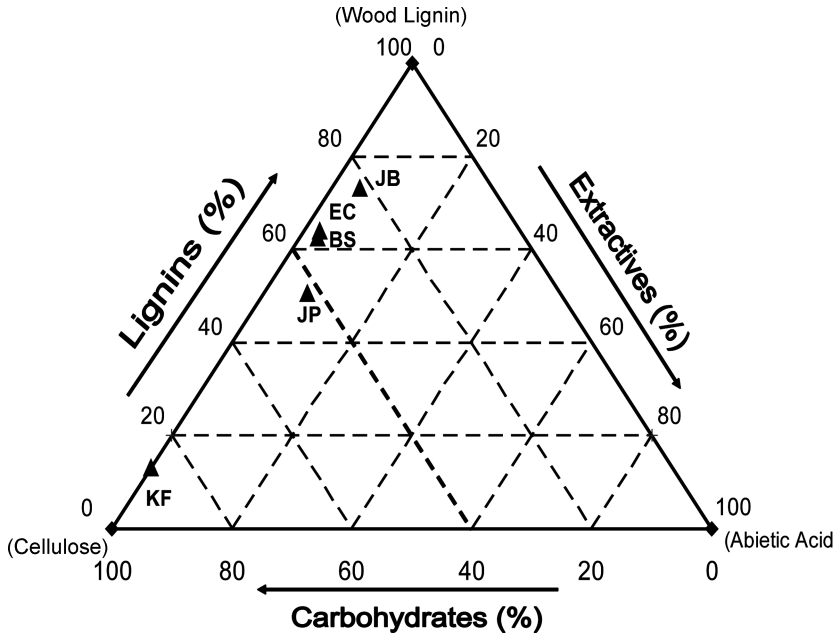

Figure 7. Ternary diagram of the surface component fraction of the used fibers (KF: bleached Kraft fiber; JP: jack pine; BS: black spruce; EC: eastern white cedar; JB: jack pine bark).

Theoretically, the atomic ratio of oxygen to carbon in pure carbohydrates (cellulose + hemicelluloses) is 0.83 and without C1 class components, while the O/C atomic ratio and C1 contribution of the resinic acids, namely abietic acid, are 0.10 and 0.95, respectively.[21,22,49] Assuming that the weight percentage of carbohydrates can be estimated according to their O/C ratio and that extractives content can be related to C1 content, then the theoretical O/C atomic value of pure cellulose and the theoretical C1 contribution in abietic acid was normalized to 100% as the maximum of carbohydrates and the maximum of extractives, respectively. Hence, a ternary diagram is used to represent the relative percentage of the three components (polysaccharides, lignin, and extractives) of all surface fibers (Figure 7).

As expected, Figure 7 indicates that the bleached Kraft fiber surface is similar to that of pure cellulose. In fact, bleached Kraft contains 87% cellulose, 13% lignin, and no extractives. The fiber surface of jack pine has more carbohydrates and less lignin than eastern white cedar and black spruce. Increasing exposure for carbohydrates means more exposure for hydroxyl groups on the fiber surface, thereby facilitating the formation of ester bonding between fibers and coupling agents during esterification (Figure 1). Eastern white

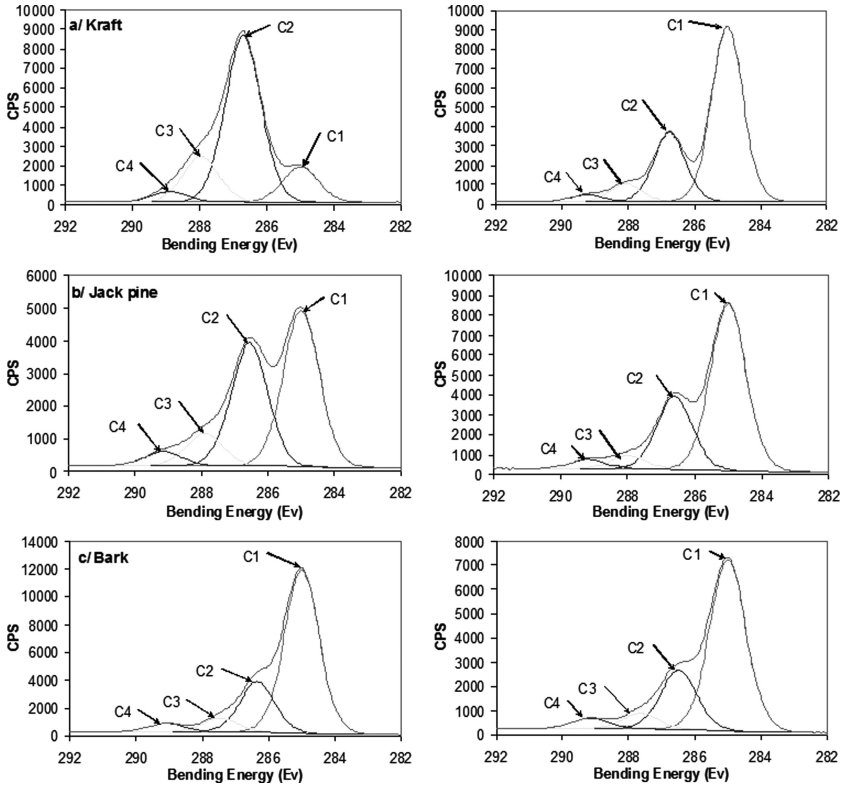

Figure 8. C1s high resolution spectra of untreated (left) and maleic polyethylene treated wood fibers (right).

cedar and black spruce fibers show approximately the same surface composition, with 34% carbohydrates, 63% lignin, and 3% extractives. However, bark fibers present the most lignin-like exposed surface, with higher content of lignin (73%) and extractives (5%). Compared to other mechanical fibers, Hua et al.[49] reported higher lignin content in CMP and CTMP surfaces, ranging from 50% to 70%.

Table 2 also presents the O/C atomic ratio and the various peak components of the carbon spectra (C1, C2, C3, and C4) for the treated fiber surfaces, while the curve fitting of the C1 high resolution spectra for untreated and maleic polyethylene treated fibers are presented in Figure 8.

As expected, treatment of bleached Kraft fibers with MAPE caused a substantial increase in carbon type C1 (C–C and/or C–H) concentration, and consequently a drastic decrease in the O/C atomic ratio (Table 2

and Figure 8a). The increased contribution of carbon type C1 and the decrease in O/C atomic ratio following the MAPE treatment might have stemmed from the aliphatic carbons in the MAPE polyethylene chains. This result clearly indicates an effective MAPE attachment to the Kraft fiber surface.

A detailed analysis of the chemical composition of the jack pine maleic polyethylene treated surface is shown in Figure 8b. The contribution of the C1 carbon atoms, which are carbon atoms bonded to carbon or hydrogen only, rose by 31.4% after MAPE treatment, whereas both the contribution of C2 carbon and the O/C atomic ratio (Table 2) dropped by 26.9% and 20%, respectively. These results indicate that unextracted jack pine fibers can react with MAPE, but at lower levels than Kraft fibers do. The observed decrease in the contribution of the C4 carbon after treatment of the jack pine fibers can be explained by the fact that the resulting ester links are masked by long polyethylene chains, so that they are not readily detected by XPS, which has a probing depth of about 5 nm.[16] It could also be explained by the greater removal of the lipohilic components from the surface during MAPE grafting conducted in a reactor in the presence of an apolair solvent (xylene).

In contrast to Kraft and jack pine fibers, bark fibers did not show a clear response to MAPE treatment (Figure 8c). The same findings were observed for unextracted eastern white cedar and black spruce fibers.

Lignin concentration variability on the wood fiber surface seems to be the major inhibitor factor for esterification. Its complex three-dimensional structure with only some available reactive hydroxyl groups largely explains its inhibition effect. Hence, based on surface lignin concentration, the fibers can be ranked by their ability to form ester bonds with MAPE as follows: Kraft >>>>>>>> jack pine >>> black spruce > eastern white cedar >>>> bark.

SEM Investigations

To corroborate the previous findings, SEM images of the MAPE modified jack pine and bark fiber surfaces are shown in Figure 9. For treated jack pine fibers, surfaces appear to be covered by polyethylene. Fiber ends and defibrillated zones are tightly covered by polyethylene. This can be explained by the S2 exposed layer, which is rich in celluloses and hemicelluloses. However, the bark fiber surfaces are fairly clean, that is, there is little plastic sticking to the bark fiber surfaces. Taken together, these images are in perfect agreement with the XPS analysis. These results partially explain why interfacial adhesion, and consequently the mechanical properties, of wood plastic composites is better for jack pine fibers than for lignin-like surface fibers (bark, eastern white cedar, and black spruce).

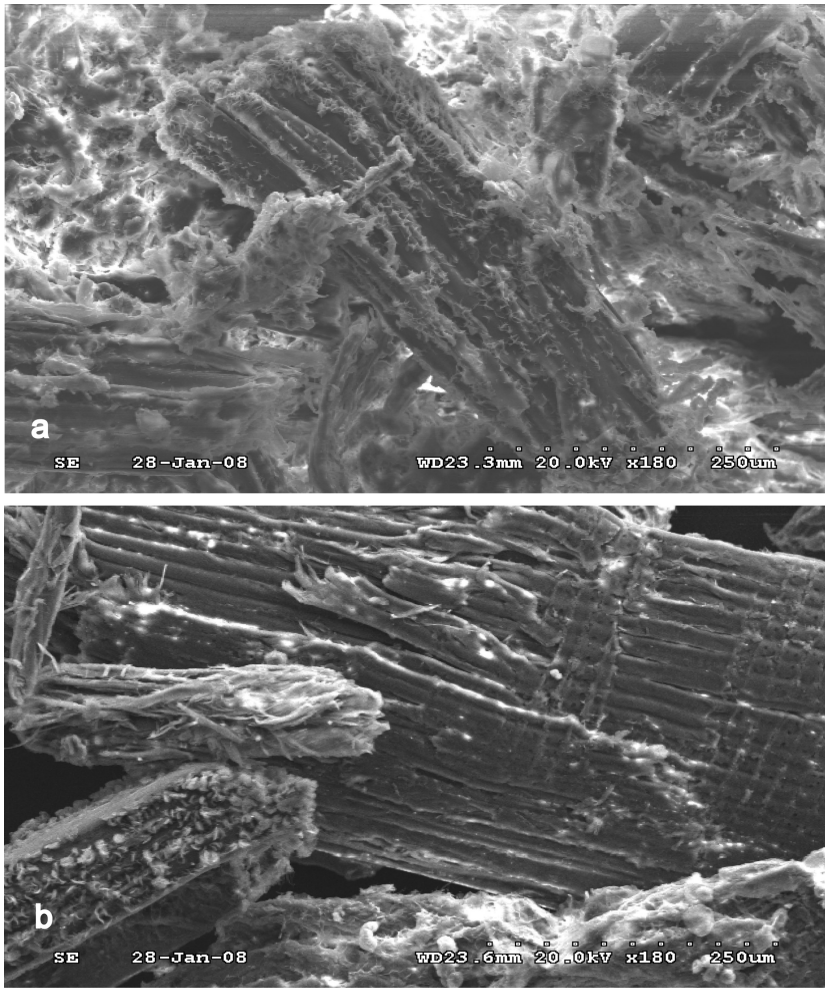

Figure 9. SEM images of MAPE treated jack pine wood fiber (a) and jack pine bark fiber (b).

CONCLUSION

DRIFTS and XPS were performed to study between-species variability in the chemical composition of wood fiber surfaces. The effect of this variability on the efficiency of the esterification reaction was also examined. Although DRIFTS was successfully used to characterize the chemical composition of the fiber surfaces, it failed to confirm esterification between unextracted wood particles and maleic polyethylene. XPS, which is a highly surface sensitive technique (10–50 Å), was more effective in detecting chemical changes in

wood fiber surfaces following MAPE treatment. XPS results were confirmed by SEM imaging. Lignin concentration variability on the fiber surface was found to be the major inhibitor factor for esterification. Jack pine fibers showed the greatest ability to form ester bonds with MAPE due to much lower surface lignin concentration. Bark fibers did not show a clear response to the MAPE treatment, using either DRIFTS or XPS.

Consequently, one of the important considerations in choosing coupling treatments is the type of wood fiber. Once the fiber surface has been clearly characterized, the concentration and chemical structure of coupling agents should be selected, as mentioned earlier.

REFERENCES

1. Rowell, R.M.; Roger, P.; Han, J.S.; Rowell, J.S.; Tshabalala, M.A. Cell wall chemistry. In *Handbook of Wood Chemistry and Wood Composites*; Rowell, R. M. (Ed.); CRC Press; Boca Raton, Fla, **2005**; 35–74.
2. Bhattacharya, A.; Misra, B.N. Grafting: A versatile means to modify polymers: Techniques, factors and applications. Progr. Polym. Sci. (Oxford). **2004**, *29*(8), 767–814.
3. Koljonen, K. Effect of surface properties of fibers on some paper properties of mechanical and chemical pulp. Dissertation for the degree of Doctor of Science in Technology. Helsinki University of Technology, department of forest product technology. Helsinki, 2004.
4. Tze, W.T.Y.; Gardner, D.J.; Tripp, C.P.; O'Neill, S.C. Cellulose fiber/polymer adhesion: Effects of fiber/matrix interfacial chemistry on the micromechanics of the interphase. J. Adhesion Sci. Technol. **2006**, *20*(15), 1649–1668.
5. Lu, J.Z.; Wu, Q. Surface and interfacial characterization of wood-PVC composite: Imaging morphology and wetting behavior. Wood Fiber Sci. **2005**, *37*(1), 95–111.
6. Luo, J.; Tang, Z.; Zhou, J. Preparation and properties of HDPE/lignin composite. Hecheng Shuzhi Ji Suliao/China Synthetic Resin and Plastics. **2006**, *23*(2), 39–42.
7. Le Digabel, F.; Averous, L. Effects of lignin content on the properties of lignocellulose-based biocomposites. Carbohydrate Polymers. **2006**, *66*(4), 537–545.
8. Saputra, H.; Simonsen, J.; Li, K. Effect of extractives on the flexural properties of wood/plastic composites. Composite Interfaces. **2004**, *11*(7), 515–524.
9. Gassan, J.; Bledzki, A.K. The influence of fiber-surface treatment on the mechanical properties of jute-polypropylene composites. Composites Part A: Appl. Sci. Manuf. **1997**, *28*(12), 1001–1005.
10. Kazayawoko, M.; Balatinecz, J.J.; Matuana, L.M. Surface modification and adhesion mechanisms in woodfiber-polypropylene composites. J. Mater. Sci. **1999**, *34*(24), 6189–6199.
11. Lu, J.Z.; Wu, Q.; Negulescu, I.I. Wood-fiber/high-density-polyethylene composites: Coupling agent performance. J. Appl. Polym. Sci. **2005**, *96*(1), 93–102.
12. Maldas, D.; Kokta, B.V.; Raj, R.G.; Daneault, C. Improvement of the mechanical properties of sawdust wood fibre-polystyrene composites by chemical treatment. Polymer. **1988**, *29*(7), 1255–1265.

13. Lu, J.Z.; Negulescu, I.I.; Wu, Q. Maleated wood-fiber/high-density-polyethylene composites: Coupling mechanisms and interfacial characterization. Composite Interfaces. **2005**, *12*(1–2), 125–140.
14. Sombatsompop, N.; Yotinwattanakumtorn, C.; Thongpin, C. Influence of type and concentration of maleic anhydride grafted polypropylene and impact modifiers on mechanical properties of PP/wood sawdust composites. J. Appl. Polym. Sci. **2005**, *97*(2), 475–484.
15. Bledzki, A.K.; Letman, M.; Viksne, A.; Rence, L. A comparison of compounding processes and wood type for wood fibre–PP composites. Composites Part A: Appl. Sci..Manuf. **2005**, *36*(6), 789–797.
16. Kazayawoko, M.; Balatinecz, J.J.; Sodhi, R.N.S. X-ray photoelectron spectroscopy of maleated polypropylene treated wood fibers in a high-intensity thermokinetic mixer. Wood Sci. Technol. **1999**, *33*(5), 359–372.
17. Kazayawoko, M.; Balatinecz, J.J.; Woodhams, R.T. Diffuse reflectance Fourier transform infrared spectra of wood fibers treated with maleated polypropylenes. J. Appl. Polym. Sci. **1997**, *66*(6), 1163–1173.
18. Chuai, C.; Almdal, K.; Poulsen, L.; Plackett, D. Conifer fibers as reinforcing materials for polypropylene-based composites. J. Appl. Polym. Sci. **2001**, *80*(14), 2833–2841.
19. Carlborn, K.; Matuana, L.M. Functionalization of wood particles through a reactive extrusion process. J. Appl. Polym. Sci. **2006**, *101*(5), 3131–3142.
20. Faix, O.; Böttcher, J.H. The influence of particle size and concentration in transmission and diffuse reflectance spectroscopy of wood. Holz als Roh–und Werkstoff. **1992**, *50*, 221–226.
21. Dorris, G.M.; Gray, D.G. The surface analysis of paper and wood fibers by ESCA I. Cellulose Chem. Technol. **1978**, *12*, 9–23.
22. Dorris, G.M.; Gray, D.G. The surface analysis of paper and wood fibers by ESCA II. Cellulose Chem. Technol. **1978**, *12*, 721–734.
23. Johansson, L.S.; Campbell, J.; Koljonen, K.; Kleen, M.; Buchert, J. On surface distributions in natural cellulosic fibres. Surf. Interface Anal. **2004**, *36*(8), 706–710.
24. Haussard, M.; Gaballah, I.; Kanari, N.; De Donato, P.; Barrès, O.; Villieras, F. Separation of hydrocarbons and lipid from water using treated bark. Water Res. **2003**, *37*(2), 362–374.
25. Pandey, K.K.; Theagarajan, K.S. Analysis of wood surfaces and ground wood by diffuse reflectance (DRIFT) and photoacoustic (PAS) Fourier transform infrared spectroscopic techniques. Holz als Roh–und Werkstoff. **1997**, *55*(6), 383–390.
26. Pandey, K.K. A study of chemical structure of soft and hardwood and wood polymers by FTIR spectroscopy. J. Appl. Polym. Sci. **1999**, *71*(12), 1969–1975.
27. Pandey, K.K.; Pitman, A.J. Examination of the lignin content in a softwood and a hardwood decayed by a brown-rot fungus with the acetyl bromide method and Fourier transform infrared spectroscopy. J. Polym. Sci., Part A: Polym. Chem. **2004**, *42*(10), 2340–2346.
28. Silverstein, R.M. *The Spectrometric Identification of Organic Compounds*; John Wiley & Sons: Hoboken, N.J., 2005.
29. Ajuong, E.M.A.; Redington, M. Fourier transform infrared analyses of Bog and modern oak wood (Quercus petraea) extractives. Wood Sci. Technol. **2004**, *38*(3), 181–190.

30. Barker, B.; Owen, N.L. Identifying softwoods and hardwoods by infrared spectroscopy. J. Chem. Educ. **1999**, *76*(12), 1706–1709.
31. Colom, X.; Carrillo, F. Comparative study of wood samples of the northern area of Catalonia by FTIR. J. Wood Chem. Technol. **2005**, *25*(1–2), 1–11.
32. Ferraz, A.; Baeza, J.; Rodriguez, J.; Freer, J. Estimating the chemical composition of biodegraded pine and eucalyptus wood by DRIFT spectroscopy and multivariate analysis. Bioresource Technol. **2000**, *74*(3), 201–212.
33. Marcovich, N.E.; Reboredo, M.M.; Aranguren, M.I. Composites from sawdust and unsaturated polyester. J. Appl. Polym. Sci. **1996**, *61*(1), 119–124.
34. Moore, A.K.; Owen, N.L. Infrared spectroscopic studies of solid wood. Appl. Spectroscopy Rev. **2001**, *36*(1), 65–86.
35. Papp, G.; Barta, E.; Preklet, E.; Tolvaj, L.; Berkesi, O.; Nagy, T.; Szatmári, S. Changes in DRIFT spectra of wood irradiated by UV laser as a function of energy. J. Photochem. Photobiol. A: Chem. **2005**, *173*(2), 137–142.
36. Ajuong, E.M.A.; Breese, M.C. Fourier Transform Infrared characterization of Pai wood (Afzelia africana Smith) extractives. **1998**, *56*(2), 139–142.
37. Brás, I.; Lemos, L.T.; Alves, A.; Pereira, M.F.R. Application of pine bark as a sorbent for organic pollutants in effluents. Manag. Environ. Qual. **2004**, *15*(5), 491–501.
38. Chen, R.; Jakes, K.A. Effect of pressing on the infrared spectra of single cotton fibers. Appl. Spectroscopy. **2002**, *56*(5), 646–650.
39. Sheshkali, H.R.Z.; Assempour, H.; Nazockdast, H. Parameters affecting the grafting reaction and side reactions involved in the free-radical melt grafting of maleic anhydride onto high-density polyethylene. J. Appl. Polym. Sci. **2007**, *105*(4), 1869–1881.
40. Nuopponen, M.H.; Birch, G.M.; Sykes, R.J.; Lee, S.J.; Stewart, D. Estimation of wood density and chemical composition by means of diffuse reflectance mid-infrared fourier transform (DRIFT-MIR) spectroscopy. J. Agricultural Food Chem. **2006**, *54*(1), 34–40.
41. Polovka, M.; Polovkova, J.; Vizárova, K.; Kirschnerova, S.; Bielikova, L.; Vrška, M. The application of FTIR spectroscopy on characterization of paper samples, modified by Bookkeeper process. Vibrational Spectroscopy. **2006**, *41*(1), 112–117.
42. Raiskila, S.; Pulkkinen, M.; Laakso, T.; Fagerstedt, K.; Löija, M.; Mahlberg, R.; Paajanen, L.; Ritschkoff, A.C.; Saranpäa, P. FTIR spectroscopic prediction of Klason and acid soluble lignin variation in norway spruce cutting clones. Silva Fennica. **2007**, *41*(2), 351–371.
43. Rodrigues, J.; Faix, O.; Pereira, H. Determination of lignin content of Eucalyptus globulus wood using FTIR spectroscopy. Holzforschung. **1998**, *52*(1), 46–50.
44. Rodrigues, J.; Puls, O.; Pereira, H. Determination of monosaccharide composition of Eucalyptus globulus wood by FTIR spectroscopy. Holzforschung. **2001**, *55*(3), 265–269.
45. Tucker, M.P.; Nguyen, Q.A.; Eddy, F.P.; Kadam, K.L.; Gedvilas, L.M.; Webb, J.D. Fourier transform infrared quantitative analysis of sugars and lignin in pretreated softwood solid residues. Appl. Biochem. Biotechnol.—Part A Enzyme Engin. Biotechnol. **2001**, *91–93*, 51–61.
46. Koubaa, A.; Riedl, B.; Koran, Z. Surface analysis of press dried-CTMP paper samples by electron spectroscopy for chemical analysis. J. Appl. Polym. Sci. **1996**, *61*(3), 545–552.

47. Kamdem, D.P.; Riedl, B.; Adnot, A.; Kaliaguine, S. ESCA spectroscopy of poly (methyl methacrylate) grafted onto wood fibers. J. Appl. Polym. Sci. **1991**, *43*(10), 1901–1912.
48. Jaic, M.; Zivanovic, R.; Stevanovic-Janezic, T.; Dekanski, A. Comparison of surface properties of beech and oakwood as determined by ESCA method. Holz als Roh– und Werkstoff. **1996**, *54*, 37–41.
49. Hua, X.; Kaliaguine, S.; Kokta, B.V.; Adnot, A. Surface analysis of explosion pulps by ESCA. Parte 1: Carbon (1s) spectra and oxygen to carbon ratios. Wood Sci. Technol. **1993**, *27*, 449–459.